

Why Do Peroxomolybdenum Complexes Chemoselectively Oxidize the Sulfur Centers of Unsaturated Sulfides and Sulfoxides? A DFT Analysis

Fabrício R. Sensato,^{*,[a]} Rogério Custodio,^[b] Elson Longo,^[c] Vicent S. Safont,^[d] and Juan Andrés^[d]

Keywords: O–O Activation / Molybdenum / Reaction mechanism / Density functional calculations / Peroxo ligands

The reasons why oxo-peroxo molybdenum complexes chemoselectively oxidize unsaturated sulfides to the corresponding sulfoxides and these to sulfones without any epoxidation of the electron-rich double bond were elucidated by transition state theory and density functional calculations at the B3LYP level. For the diperoxo model complex with the structure $\text{MoO}(\eta^2\text{-O}_2)_2\text{OPH}_3$ and for allyl methyl sulfide as a model of unsaturated sulfides, the calculations show that the oxygen transfer process from the peroxomolybdenum complex to the sulfur center requires a lower free activation energy ($\Delta G^\ddagger = 19.0 \text{ kcal mol}^{-1}$) than the attack on the double bond moiety ($\Delta G^\ddagger = 26.4 \text{ kcal mol}^{-1}$) of the unsaturated sulfide. Subsequent oxidation of allyl methyl sulfoxide at the sulfinyl group to yield the corresponding sulfone also requires a lower activation energy ($\Delta G^\ddagger = 21.5 \text{ kcal mol}^{-1}$) than the corresponding epoxidation process ($\Delta G^\ddagger = 27.7 \text{ kcal mol}^{-1}$),

yielding 2,3-epoxypropyl methyl sulfoxide. These results unambiguously account for these complexes' excellent chemoselectivity towards the sulfur groups in unsaturated sulfides and sulfoxides, as has been observed experimentally. On the basis of SCRF calculations, the level of chemoselectivity is predicted to diminish with increasing solvent polarity. Charge decomposition analysis and the orbital interaction model reveal that unsaturated sulfides with reaction sites carrying lone pair and π electrons behave as nucleophiles toward the electrophilic peroxo oxygen group. The origin of the chemoselectivity is ascribed to the fact that the electronic state related to the sulfur lone pair (HOMO) lies 1.2 eV above that associated with the π electrons (HOMO–1).

(© Wiley-VCH Verlag GmbH & Co. KGaA, 69451 Weinheim, Germany, 2005)

Introduction

The conversion of organic sulfides into sulfoxides and sulfones has attracted considerable interest due to their use in a wide range of applications, including industrial processes.^[1] A prominent sulfide oxidation process should allow control of the degree of product oxidation (that is, whether either a sulfoxide or sulfone is obtained). It is usually also desirable that such a method should demonstrate tolerance towards a variety of functional groups, which should remain unchanged during the oxidation process.

In search of a catalytic process meeting these requirements, Cass et al.^[2] have examined the use of Mimoun-type^[3] complexes $\text{MoO}(\text{O}_2)_2(\text{L})(\text{H}_2\text{O})$ (L = pyridine *N*-oxide or pyrazole) to oxidize a wide variety of substituted sul-

fides such as, among others, aliphatic and aromatic sulfides, ketosulfides, and olefinic sulfides. In addition to establishing the conditions that allow mild oxidation of sulfides to sulfoxides (avoiding overoxidation to sulfones), they observed excellent chemoselectivity of these complexes toward the sulfur groups of functional sulfides or sulfoxides in which another substituent susceptible to oxidation, such as an unsaturated bond, was also present. As an example, if the conditions are not mild, olefinic sulfides are chemoselectively oxidized to the corresponding sulfones, with no epoxy byproducts even in the presence of an excess of oxidant.^[2]

It has also been reported that a parent complex $\text{MoO}(\text{O}_2)_2(\text{hmpa})(\text{H}_2\text{O})$ (hmpa = hexamethylphosphoric triamide) oxidizes dibenzyl and phenyl vinyl sulfides to their sulfones.^[4] These results are surprising, since well known conventional oxidants are unable to convert unsaturated sulfides selectively to the corresponding sulfoxides or sulfones, due to the interference of electron-rich double bonds. It is worth noting that, in addition to its cost-effectiveness, the oxidation method mediated by peroxomolybdenum is environmentally benign, inasmuch as the complex can be stoichiometrically recovered in the presence of hydrogen peroxide and reused to oxidize a new batch of substrates, showing similar catalytic efficiency and yielding

[a] Centro Universitário Fundação Santo André, Av. Príncipe de Gales, 821, 09060–650, Santo André, Brazil
fabricao.sensato@fsa.br

[b] Instituto de Química, Universidade Estadual de Campinas, CP 6154, 13084–971, Campinas, Brazil

[c] Departamento de Química, Universidade Federal de São Carlos, CP 676, 13565–905, São Carlos, Brazil

[d] Departament de Ciències Experimentals, Universitat Jaume I, Apartat 224, 12080, Castelló, Spain

Supporting information for this article is available on the WWW under <http://www.eurjoc.org> or from the author.

water as by-product. As far as the tolerance of unsaturated bonds is concerned, molybdenum peroxo complexes have also been reported to be able to catalyze the isomerization of some allylic alcohols^[5] and the oxidation of allylbenzenes to the corresponding alcohols and ketones.^[6]

The process of epoxidation of olefins by Mimoun-type peroxo complexes $[\text{Mo}(\text{O}_2)_2\text{L}_x]$ ($\text{M} = \text{Mo}, \text{W}$ and donor ligand $\text{L} = \text{pyridine}, \text{dimethylformamide}, \text{hexamethylphosphoric triamide}$, among others; $x = 1, 2$) has been the object of a large number of experimental^[7,8] and theoretical studies.^[9] Two main hypothesis have dominated the discussions. The first is due to Mimoun,^[3] who suggested that the olefin coordinates to the metal center prior to subsequent insertion into the $\text{Mo}-\text{O}$ bond, forming a five-member metallacycle. On the other hand, Sharpless suggested a concerted reaction mechanism involving a direct transfer of the peroxo oxygen to the olefin through a three-membered ring.^[10] Recent computational studies^[9d,9g] indicated the latter mechanism to be favored in this reaction.

It is now recognized that metal peroxo complexes are very versatile oxygen transfer agents in the oxidation of sulfides or sulfoxides.^[11] However, the mechanism for this oxidation is less understood and only a few theoretical studies have been reported, in marked contrast to the mechanism for the epoxidation of olefin catalyzed by metal peroxo complexes. The mechanism of the oxidation of bis(*tert*-butyl) disulfide by a comparable vanadium peroxo complex was recently theoretically investigated by Maseras et al.^[12] We have for the first time reported a theoretical study of the molecular mechanism of the oxidation of sulfides/sulfoxides to sulfoxides/sulfones by mono- and diperoxo complexes of molybdenum.^[13] Besides unveiling the corresponding molecular mechanism, we addressed the relative nucleophilicity/electrophilicity of the sulfide vs. its sulfoxide, since the difference in the degree of nucleophilicity/electrophilicity of these functional groups has been widely explored to assess the electronic nature of oxygen transfer reactions.^[11b,14]

Here we report a density functional study on the mechanism of oxidation of unsaturated sulfides by peroxomolybdenum complexes. The emphasis is on the factors controlling its inherent chemoselectivity as far as the competition between sulfur group oxidation and double bond epoxidation is concerned. We have analyzed the origin of chemoselectivity on the basis of calculated free energy profiles, charge decomposition analysis (CDA), natural atomic charges, and orbital interactions. It is hoped that the theoretical calculations presented in this paper, together with the available experimental data, will improve understanding of the molecular mechanism of this type of chemical process.

Results and Discussion

To make the theoretical study feasible, the parent complex $\text{MoO}(\text{O}_2)_2\text{OPH}_3$ was used to represent the peroxomolybdenum complex,^[15] with L modeled by an $-\text{OPH}_3$ ligand.

We assumed the reaction obeys the Sharpless mechanism and that a peroxo oxygen atom *trans* to the phosphane oxide ligand is transferred to the substrate. These assumptions are based on previous theoretical studies, which showed that the transfer process of a *trans* oxygen atom from diperoxo complexes of transition metals to olefins requires a lower activation energy than when the process involves the *cis* oxygen.^[9d,9g,16] With regard to the sulfide/sulfoxide oxidation by peroxo molybdenum complexes, this assumption is further supported by experimental results ruling out any coordination process between the substrate and the oxidant.^[11a,11e] It should be mentioned that direct oxygen transfer was recently predicted to be the ruling channel in the oxidation of sulfides by vanadium peroxo complexes and that no insertion mechanism was successfully characterized.^[12] The allyl methyl sulfide was selected as a representative model of functional sulfides, in that it contains two competing oxidizable centers. The oxidant can thus attack this molecule either at the double bond (process **I**, via TS1), yielding the corresponding epoxide (2,3-epoxypropyl methyl sulfide), or at the sulfur center (process **II**, via TS2), to yield the corresponding sulfoxide (allyl methyl sulfoxide). For purposes of comparison, we also investigated the oxidation both of ethylene (process **III**, via TS3) and of dimethyl sulfide (process **IV**, via TS4) by $\text{MoO}(\text{O}_2)_2\text{OPH}_3$. In all of these processes, the diperoxo species $\text{MoO}(\text{O}_2)_2\text{OPH}_3$ is transformed into the monoperoxo form ($\text{MoO}_2(\text{O}_2)-\text{OPH}_3$). Monoperoxo complexes were also found to be active species in the oxidation of sulfides, and more detailed information is given elsewhere.^[13] The calculated structures of reactants and products are depicted in Figure 1.

Free Energy Profiles

Selected thermodynamic and activation parameters for these processes are given in Table 1, while the corresponding transition structures are depicted in Figure 2. Detailed structural descriptions of all TSs as well as reactants and products are given in the Supporting Information.

Analysis of the results given in Table 1 shows the oxidations to be exergonic processes, and the corresponding ΔG° values lie within a narrow range from -33.5 to $-34.4 \text{ kcal mol}^{-1}$. However, the oxidations at the sulfur centers (reactive pathways **II** and **IV**) are much more favorable processes from a kinetic point of view ($\Delta G^\ddagger = 19.0$ and $18.5 \text{ kcal mol}^{-1}$, respectively) than the epoxidation of the double bonds (channels **I** and **III**; $\Delta G^\ddagger = 26.4$ and $28.2 \text{ kcal mol}^{-1}$, respectively). These results clearly explain the experimentally observed excellent chemoselectivity of these complexes toward the sulfur groups of unsaturated sulfides. A comparison of values of the activation parameters ΔH^\ddagger and $-T\Delta S^\ddagger$ reveals that the entropic contributions are very similar for all four cases, so it is to be expected that chemoselectivity should not be influenced significantly by temperature variations and that inherent chemoselectivity should be related mainly to the enthalpic term.

Although allyl methyl sulfoxide is kinetically the most favored product of oxidation of allyl methyl sulfide oxi-

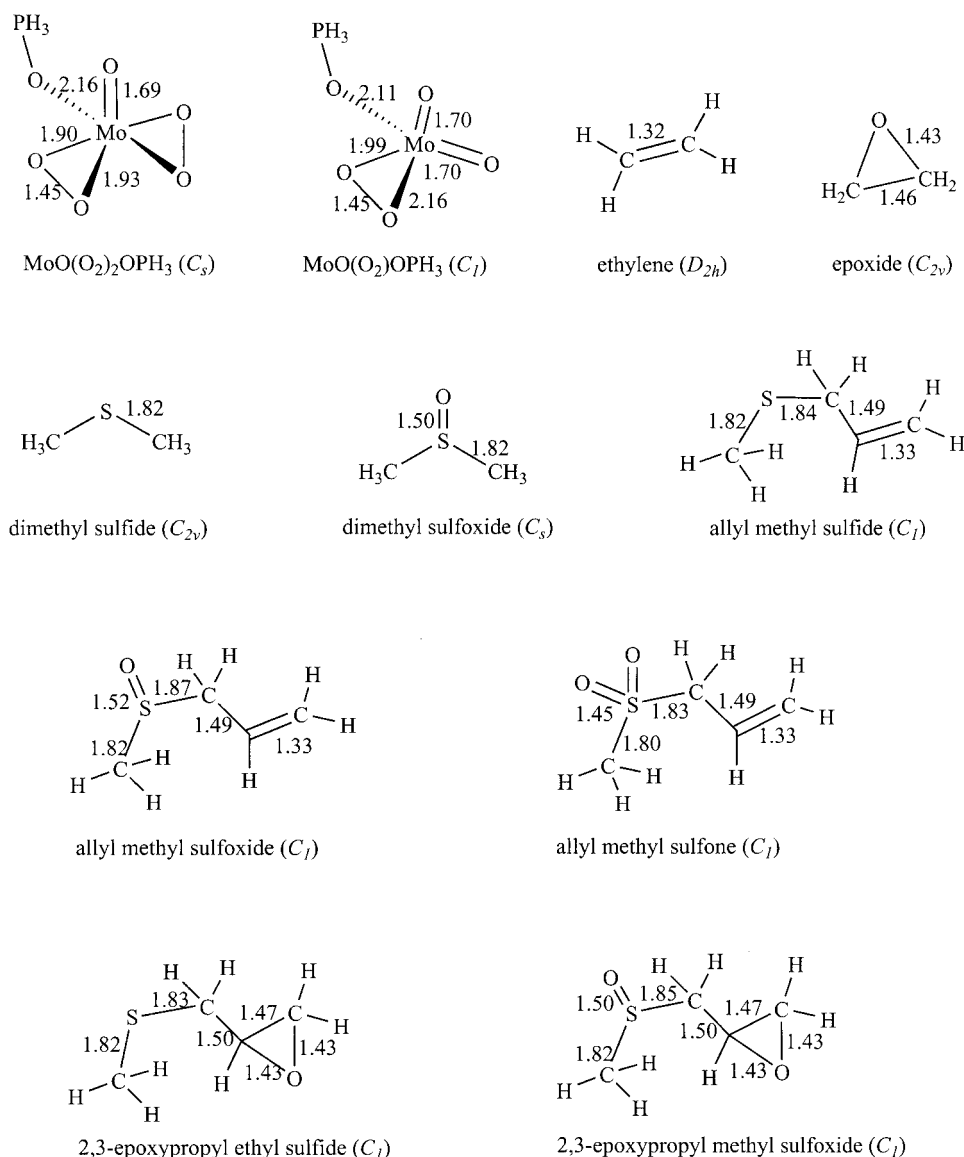


Figure 1. Calculated molecular structures of reactants and products.

Table 1. Calculated thermodynamic (ΔG°) and activation parameters (kcal mol⁻¹) and localization parameter (x^\ddagger) for processes I–IV.

Process	ΔG°	ΔH^\ddagger	$-T\Delta S^\ddagger$	ΔG^\ddagger	x^\ddagger
I	-34.4	14.7	11.7	26.4	0.302
II	-33.5	7.6	11.4	19.0	0.244
III	-34.0	17.8	10.4	28.2	0.314
IV	-33.6	7.6	10.9	18.5	0.242

dation by the peroxomolybdenum complex (by process II), it still presents two sites susceptible to oxidation: namely, the allyl and the sulfinyl groups. Thus, this compound can be further oxidized by another MoO(O₂)₂OPH₃ complex to yield 2,3-epoxypropyl methyl sulfoxide (process V, via TS5) or allyl methyl sulfone (process VI, via TS6). These two reactive channels were also examined; Table 2 shows their cal-

culated kinetic and thermodynamic parameters. For purposes of comparison, oxidation of dimethyl sulfoxide was also included (process VII, via TS7). The main structural characteristics relating to the corresponding transition structures are shown in Figure 3.

Analysis of Table 2 reveals that, both from the thermodynamic and from the kinetic perspectives, MoO(O₂)₂OPH₃ preferentially attacks the allyl methyl sulfoxide at the sulfinyl group ($\Delta G^\circ = -52.8$ and $\Delta G^\ddagger = 21.5$ kcal mol⁻¹) rather than at the allylic one ($\Delta G^\circ = -34.4$ and $\Delta G^\ddagger = 27.7$ kcal mol⁻¹), yielding the corresponding sulfone. These results are summarized in the free energy profile in Figure 4. Our findings are in line with experimental results, since the oxidation of unsaturated (or not) sulfide by peroxomolybdenum complexes under less mild reaction conditions is reported not to stop at the sulfoxide stage, yielding the corresponding sulfones as the main products.^[2,4]

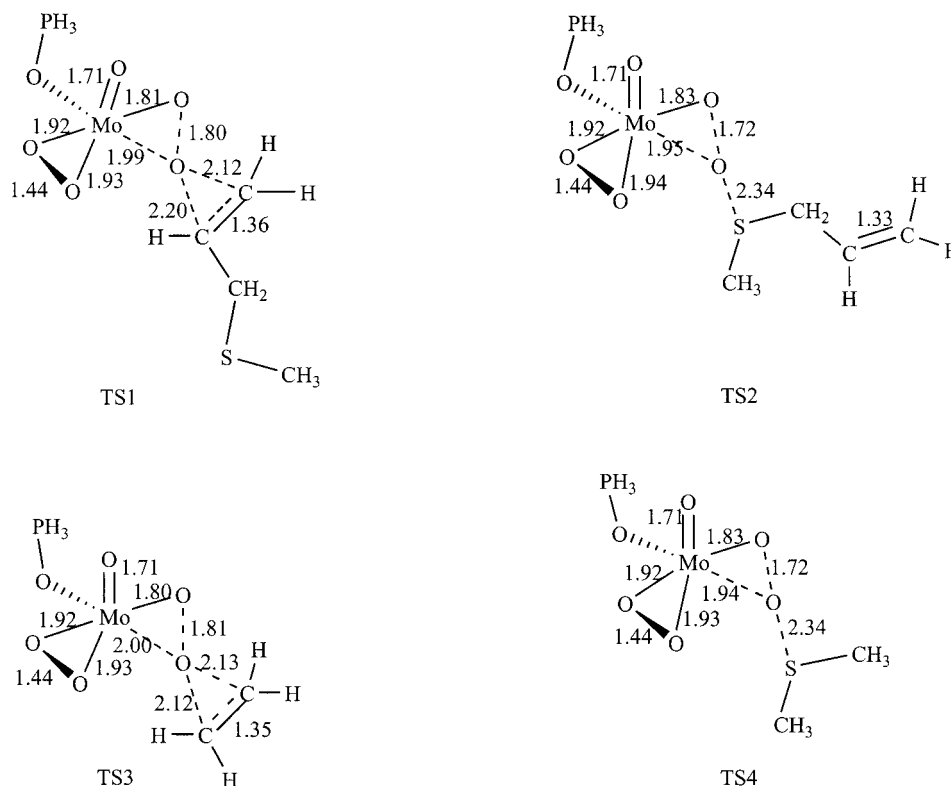


Figure 2. Calculated transition structures for the oxygen transfer process from peroxomolybdenum complex to allyl methyl sulfide (into the electron-rich double bond via TS1 or into the sulfur center via TS2), to ethylene (via TS3), and to dimethyl sulfide (via TS4).

Table 2. Calculated thermodynamic (ΔG°) and activation parameters (ΔH^\ddagger , $-T\Delta S^\ddagger$) and localization parameters (x^\ddagger) for processes V–VII.

Process	ΔG°	ΔH^\ddagger	$-T\Delta S^\ddagger$	ΔG^\ddagger	x^\ddagger
V	–34.4	16.6	11.1	27.7	0.312
VI	–52.8	10.6	10.5	21.5	0.281
VII	–53.1	9.2	11.4	20.6	0.272

Analysis of ΔG° and ΔG^\ddagger values of channels belonging to similar processes shows that they all obey the Bell–Evans–Polanyi principle to some extent, since product stabilization induces stabilization of the transition structure. For the channels I and III, which correspond to the attack of the alkenyl group on the peroxo oxygen, the ΔG° values are –34.4 to –34.0 kcal mol^{–1}, respectively, whereas the corresponding ΔG^\ddagger values are 26.4 and 28.2 kcal mol^{–1}. For channels II and IV, in which the peroxo oxygen is attacked by the sulfur group of the substrate, the ΔG° values are –33.5 and –33.6 kcal mol^{–1}, respectively, and the corresponding ΔG^\ddagger values are 19.0 and 18.5 kcal mol^{–1}. Finally, the ΔG° values for the channels VI and VII, relating to the direct attack of the sulfinyl group on the peroxo oxygen, are –52.8 and –53.1 kcal mol^{–1}, respectively, and the corresponding ΔG^\ddagger values are 21.5 and 20.6 kcal mol^{–1}. We want to point out, however, that the Bell–Evans–Polanyi principle fails for the cases in which the oxygen transfer processes to sulfur or sulfinyl groups are directly compared (i.e., the oxidation of the sulfides is thermodynamically less but kinetically more favorable than that of the correspond-

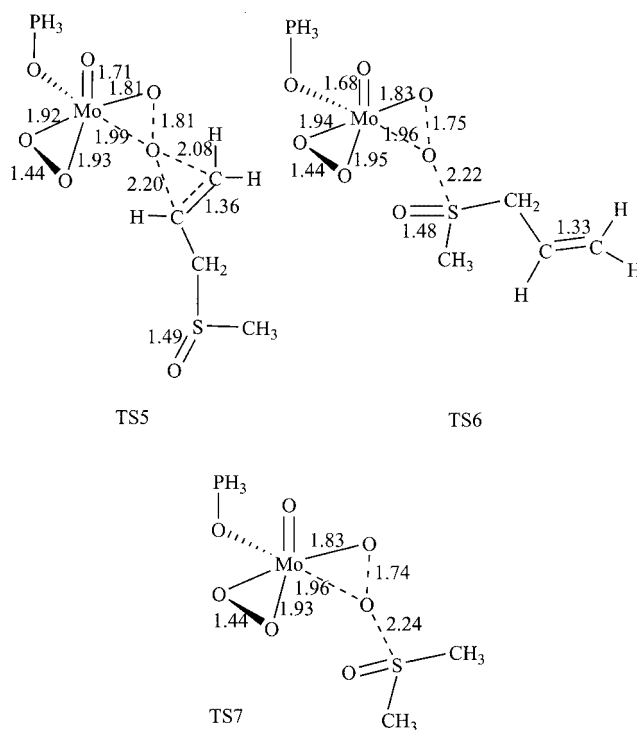


Figure 3. Calculated transition structures for the oxygen transfer process from peroxomolybdenum complex to allyl methyl sulfoxide (into its electron-rich double bond, via TS5, or into its sulfinyl group, via TS6) and to the dimethyl sulfoxide, via TS7.

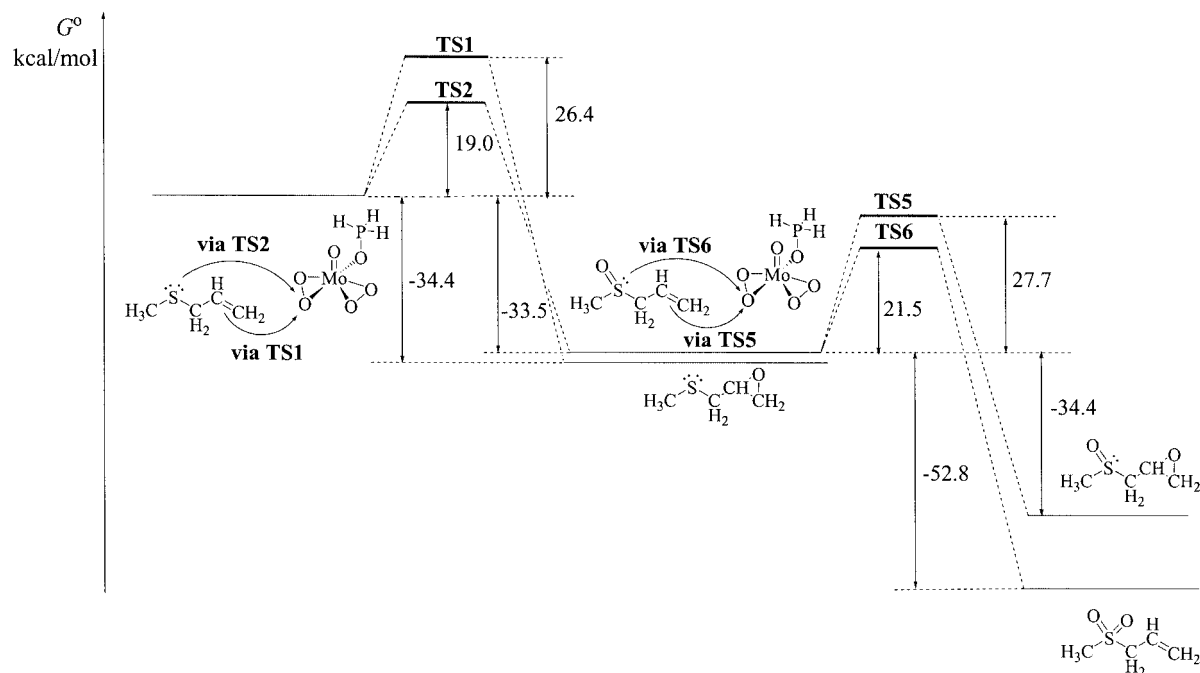


Figure 4. Free energy profile for consecutive oxygen transfers from peroxomolybdenum complexes to an allyl methyl sulfide molecule.

ing sulfoxides, as can be noted by comparing channels II and VI with IV and VII).

Solvent Effects

Calculated barrier energies were further refined by the addition of solvent effects (with the gas geometries) by the SCRF approach.^[17] Consistently with conventional reaction procedures employed in the oxidation of alkenes and sulfides by Mimoun-type complexes, solvent effects (dielectric constant ϵ in parentheses) were considered for: chloroform^[8d,11b,11c] ($\epsilon = 4.9$), dichloroethane (DCE)^[11a] ($\epsilon = 10.36$), and acetonitrile^[2] ($\epsilon = 36.64$). Table 3 presents the activation energy variation $\Delta\Delta E^\ddagger$ induced by solvent effects on channels I, II, V, and VI. For all cases investigated, solvent effects were found to stabilize both the reactants and the transition structure. However, the stabilization of reactants is larger than that of the corresponding TSs, so solvent effects are found to increase the activation energies for all pathways considered.

Table 3. Activation energy increase ($\Delta\Delta E^\ddagger$) induced by solvent effects (values are given in kcal mol⁻¹).

Channel	$\Delta\Delta E^\ddagger$ (CHCl ₃)	$\Delta\Delta E^\ddagger$ (DCE) ^[a]	$\Delta\Delta E^\ddagger$ (CH ₃ CN)
I	1.7	2.0	2.1
II	2.3	2.7	3.0
V	2.2	2.6	2.8
VI	2.7	3.2	3.5

[a] Dichloroethane.

For all system considered, the activation barriers increase with increasing solvent polarity (see Table 3). Consistently

with this, it has been shown experimentally that the epoxidation of similar olefins with a parent complex $\text{MO}(\text{O}_2)_2\text{-HMPT}$ in alcohol as solvent is much slower than in DCE.^[18] It should be mentioned that solvent effects were found to be dependent on the nature of the donor ligand bonded to the metal center, as revealed recently in a theoretical study of solvent effects on olefin epoxidation by Hermann-type complexes $\text{CH}_3\text{ReO}(\text{O}_2)_2(\text{L})$: for $\text{L} = \text{pyridine}$ or pyrazole , the activation barrier increases as solvent polarity increases, whereas the opposite behavior is predicted for $\text{L} = \text{H}_2\text{O}$.^[19] We want to emphasize, however, that short-range (chemical) interaction of the solute with solvent molecules is not taken into account in polarizable continuum models, so the model's limitations should be kept in mind when analyzing the present results.

As far as solvent effects on chemoselectivity are concerned, Table 3 shows that, for all the solvents considered, the increase in the activation barrier in TS2 due to the solvent effect is slightly greater than that in TS1 for all solvents considered. Furthermore, the difference increases with increasing solvent polarity, peaking at 0.9 kcal mol⁻¹ for acetonitrile. This value represents about 12% of the difference between the activation barriers of TS1 and TS2. As a consequence, solvent effects as considered here are predicted to diminish the level of chemoselectivity in the oxidation of unsaturated sulfides to sulfoxides by molybdenum diperoxo complexes. The origin of the solvent's influence on the chemoselectivity can be understood in terms of the stabilization of the corresponding TSs. The calculated dipole moment is 6.3 D for TS1 and 4.1 D for TS2, so it can be expected that polar solvents should stabilize TS1 more efficiently than TS2, and thus diminish the level of chemoselectivity.

Calculated Structures of TSs

The transition structures were found to exhibit spiro orientations in which the oxidizable fragment (alkenyl, sulfinyl or sulfur groups) is almost orthogonal to the plane formed by the peroxo group and the metal center (see Figure 1 for TS1–TS4 and Figure 2 for TS5–TS7).

Common structural characteristics relating to the formation of all TSs include the elongation of the attacked O–O peroxo bond, a decrease in the Mo–O_{cis} distance (where O_{cis} represents the oxygen atom *cis* to the ligand), and a less noticeable enlargement in the Mo–O_{trans} distance (O_{trans} is the attacked oxygen atom *trans* to the ligand). The magnitudes of the structural variations in corresponding TSs are summarized in Table 4, in which the data are arranged by magnitude rather than by TS labels, in order to make the tendencies clearer. The first three TSs (TS3, TS1, and TS5) correspond to those in which the peroxo group is attacked by the alkenyl moiety. The next two, TS6 and TS7, correspond to attack by the sulfinyl group, and in the last two transition structures, TS2 and TS4, by the sulfur group.

Table 4. Main structural variations relating to the formation of TSs.

TS	$\Delta(\text{O–O})$	$\Delta(\text{Mo–O}_{\text{cis}})^{[a]}$	$\Delta(\text{Mo–O}_{\text{trans}})^{[b]}$
TS3	0.36	–0.12	0.07
TS1	0.35	–0.11	0.06
TS5	0.35	–0.11	0.06
TS6	0.30	–0.11	0.03
TS7	0.29	–0.09	0.03
TS2	0.27	–0.09	0.02
TS4	0.27	–0.09	0.01

[a] Mo–O_{cis} bond *cis* to the ligand. [b] Mo–O_{trans} bond *trans* to the ligand.

Analysis of the results presented in Table 4 shows that, in general, the greater the elongation of the O–O distance, the greater the increase in the Mo–O_{trans} bond length and the greater the contraction of the Mo–O_{cis} bond. The elongation of O–O is associated with the charge transfer from the substrate to the unoccupied $\sigma^*(\text{O–O})$ level of the molybdenum peroxo complex, as discussed below. The shortening of the Mo–O_{cis} bond is related to its conversion into a Mo=O bond, as confirmed by an IRC calculation. The most important changes occur in the peroxo group. When the peroxo oxygen group is attacked by the alkenyl moiety (TS1, TS3, and TS5) the O–O distance is elongated by 0.35 Å. In TS6 and TS7 (attack by the sulfinyl group), the O–O distance increases by about 0.30 Å, and it is increased by 0.27 Å in TS2 and TS4, under the attack of the sulfur group. This behavior correlates with the electrophilic character of these reactions, as discussed below.

The S–O–O bond angles in the transition structures TS2 and TS4 (sulfide oxidation), and in TS6 and TS7 (sulfoxide oxidation) are nearly 180 degrees. It is thus convenient to define the localization parameter of the transition structures along the reaction coordinate (x^\ddagger) in terms of the O–O peroxo bond length and the S–O bond length. The localization parameter is therefore defined as follows [Equation (1)].

$$x^\ddagger = \frac{d(\text{O–O})_{\text{TS}} - d(\text{O–O})_{\text{REACT}}}{d(\text{O–O})_{\text{TS}} - d(\text{O–O})_{\text{REACT}} + d(\text{O–O})_{\text{TS}} - d(\text{O–O})_{\text{PROD}}} \quad (1)$$

where $d(\text{O–O})_{\text{TS}}$ and $d(\text{O–O})_{\text{REACT}}$ are the peroxo bond lengths in the TS and in the peroxo molybdenum complex, respectively, and $d(\text{S–O})_{\text{TS}}$ and $d(\text{S–O})_{\text{PROD}}$ are the distances between the sulfur and the oxygen atoms in the TS and in the product, respectively. The localization parameter x^\ddagger for the epoxidation of the unsaturated moiety (via TS1, TS3, and TS5) was calculated in a similar way: $d(\text{S–O})_{\text{TS}}$ and $d(\text{S–O})_{\text{PROD}}$ were substituted by the distance between the double bond and the attacked peroxo oxygen in the corresponding TS and product, respectively.

Except for TS5 (see Table 1 for TS1–TS4 and Table 2 for TS5–TS7), it may be noted that, for a given oxidizable moiety (i.e., whether the attacked oxidation site is a sulfur, sulfinyl, or alkenyl group), the more exergonic reactions have earlier transition structures than the less exergonic ones. Thus, TS1 ($\Delta G^\circ = -34.4 \text{ kcal mol}^{-1}$, $x^\ddagger = 0.302$) is found to be earlier than TS3 ($\Delta G^\circ = -34.0 \text{ kcal mol}^{-1}$, $x^\ddagger = 0.314$), TS2 ($\Delta G^\circ = -33.5 \text{ kcal mol}^{-1}$, $x^\ddagger = 0.244$) is slightly later than TS4 ($\Delta G^\circ = -35.6 \text{ kcal mol}^{-1}$, $x^\ddagger = 0.242$), and TS6 ($\Delta G^\circ = -52.8 \text{ kcal mol}^{-1}$, $x^\ddagger = 0.281$) is later than TS7 ($\Delta G^\circ = -53.1 \text{ kcal mol}^{-1}$, $x^\ddagger = 0.272$). Therefore, the Hammond postulate and the Bell–Evans–Polanyi principle appear to be reasonably useful for predicting qualitative changes in the reactivity of these systems. The particular behavior of TS5 is addressed below.

It should be noted that the molecular structures of the substrate molecules are only slightly modified in the corresponding transition structures in comparison to those of the free species. The C–C distances in TS1, TS3 and TS5, for instance, are calculated to be approximately 0.03 Å longer than the C–C distance in the ethylene molecule.

Charge Decomposition Analysis and Orbital Interaction Model

We recently used the CDA approach to gain insight into the electronic character of the oxygen transfer processes from mono- and diperoxo molybdenum complexes to unsubstituted sulfides or sulfoxides (i.e., whether the oxidant attacks the substrate in an electrophilic or nucleophilic way). Our results showed that the molybdenum peroxo complex behaves as the electrophilic partners in these reactions, but they are more strongly electrophilic oxidants towards sulfides than they are towards sulfoxides. Moreover, the predominant orbital interaction involves an electron transfer from the HOMO of the substrate to the $\sigma^*(\text{O–O})$ level of the oxidant.^[13]

In this study we used the CDA to gain an insight into the origin of the chemoselectivity in the oxidation of unsaturated sulfides by the peroxo molybdenum complex. In CDA, the interaction between the occupied orbitals of the oxidizable substrate and the vacant orbitals of the oxidant is defined as donation (*d*), back-donation (*b*) is the interaction of the occupied orbitals of the oxidant and the vacant

Table 5. NBO charges (q) and Charge Decomposition Analysis (CDA) terms (d , b , d/b , r , and Δ) for processes I–VII.

Process	$q^{[a]}$	d	b	d/b	r	Δ
I	0.33	0.229	0.121	1.89	−0.241	−0.008
II	0.34	0.168	0.082	2.05	−0.209	−0.007
III	0.33	0.231	0.129	1.79	−0.259	−0.007
IV	0.34	0.161	0.076	2.12	−0.210	−0.002
V	0.32	0.228	0.134	1.70	−0.258	−0.008
VI	0.38	0.212	0.141	1.50	−0.202	−0.016
VII	0.37	0.200	0.128	1.56	−0.206	−0.013

[a] Natural orbital charges at the oxidizable substrate along TS1–TS7.

orbitals of the oxidizable substrate, and r is the interaction between occupied orbitals of both oxidant and substrate. The d/b ratio is a measure of the electronic character of the oxidant. If $d/b > 1$ the oxidant is electrophilic, whereas if $d/b < 1$ it is a nucleophilic one.^[9e] Small values of rest terms (Δ) indicate that the electronic structures of TSs may be properly described in terms of donor–acceptor interactions. The main CDA parameters for TS1–TS7 are summarized in Table 5. From a CDA standpoint, all the processes investigated here take place through electrophilic attack by the metal peroxide on the organic substrate ($d/b > 1$). Oxygen transfer to the sulfur groups of sulfides is the most electrophilic process (TS2: $d/b = 2.05$; TS4: $d/b = 2.12$), while oxidation of the sulfinyl groups of sulfoxides is the least electrophilic (TS6: $d/b = 1.50$; TS7: $d/b = 1.56$). The epoxidation of the double bond exhibits an intermediary electrophilic character (TS1: $d/b = 1.87$; TS3: $d/b = 1.79$; TS5: $d/b = 1.70$). The electrophilic character of these reactions is also corroborated by the calculated NBO charges at the oxidizable substrate in the corresponding transition structures (see Table 5), which indicate a charge transfer process from the substrate to the molybdenum peroxo complex.

In TS1, TS3, and TS5, the main orbital interaction takes place between the $\sigma^*(\text{O–O})$ level of the peroxomolybdenum complex and the $\pi(\text{C–C})$ state of the substrate. The $\pi(\text{C–C})$ state is associated with the HOMO in the ethylene molecule, but it is the main component in the HOMO–1 of allyl methyl sulfide and allyl methyl sulfoxide. The $\sigma^*(\text{O–O})$ orbital of peroxomolybdenum interacts with the HOMO of the sulfide (sulfur p orbital related to its lone pair) in TS2 and TS4. The interaction between the $\sigma^*(\text{O–O})$ of peroxomolybdenum and the HOMO of the corresponding sulfoxide (an admixture of s sulfur and $\pi^*(\text{S=O})$ orbitals) is predominant in TS6 and TS7.

As mentioned above, the dominant interaction of donation in TS1 is between the HOMO–1 of the allyl methyl sulfide, the greatest contributions of which are associated with the bonding $\pi(\text{C–C})$ orbital, and the unoccupied $\sigma^*(\text{O–O})$ level of the peroxomolybdenum. On the other hand, the dominant orbital interaction in TS2 occurs between the HOMO of allyl methyl sulfide (predominantly constituted of sulfur atom p orbital) and the $\sigma^*(\text{O–O})$ level of the oxidant. The main orbital interactions in TS1 and TS2 are depicted in Figure 5. Given that these processes may be regarded as donor–acceptor interactions, as indicated by the small values of the rest terms (Δ), and since their corresponding TSs are found to be early-type along

the reaction coordinates, the origin of chemoselectivity may be interpreted in terms of the electronic structures of the reactants. The HOMO of allyl methyl sulfide is calculated to be ca. 1.2 eV higher than the HOMO–1. Since it is concentrated mainly in the sulfur atom, the electrophilic attack of an oxidant on the sulfur atom would be expected to be favored over the attack on the allylic group in the unsaturated sulfide oxidation process. This view may be further explored to estimate the influence of substituents on the chemoselectivity of the oxidation of unsaturated sulfides by metal peroxo complexes, without explicitly locating the transition structure (as long as other effects, such as steric ones, may be neglected). For a given unsaturated sulfide, it is sufficient to calculate the energy gap between the orbital related to the bonding $\pi(\text{C–C})$ orbital and that related to the sulfur's lone pair. Substituents yielding the smaller energy gap will decrease the level of chemoselectivity.

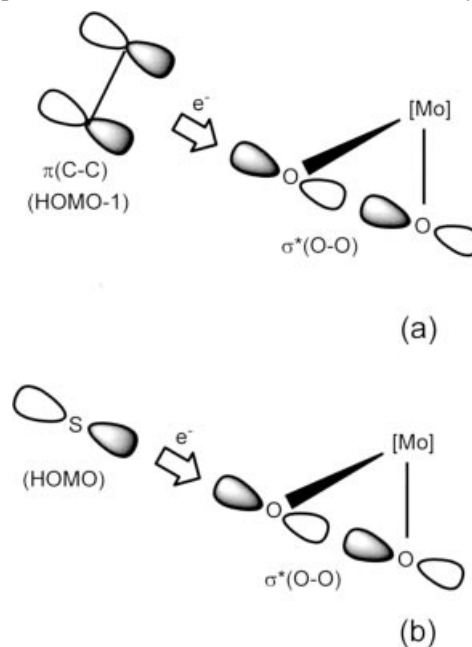


Figure 5. Predominant orbital interaction of charge transfer in the transition states relating to the allyl methyl sulfide oxidation with peroxomolybdenum complex yielding: a) 2,3-epoxypropyl methyl sulfide, via TS1, and b) allyl methyl sulfoxide, via TS2. The $\pi(\text{C–C})$ bond is the main constituent of the HOMO–1 of allyl methyl sulfide, while the p orbital of the sulfur atom is the main component of its HOMO.

Exploring the electrophilic nature of the oxygen transfer reaction from metal peroxo complexes to olefins, Rosch and

co-authors found a linear correlation between the energy of the olefin HOMO and the activation barrier: the higher the energy of the olefin HOMO, the lower the corresponding activation barrier.^[90,20] In this study we extend this frontier orbital argument by taking account of the dominant orbital interaction in each transition structure investigated. Thus, it is expected that the activation barriers should correlate with the energy of the substrate's HOMO in TS2, TS3, TS4, TS6, and TS7, and with that of the substrate's HOMO-1 in TS1 and TS5.

Figure 6 shows how the activation free energies (ΔG^\ddagger) correlate with the energy of the substrate's orbital involved in the predominant orbital interaction in the corresponding TSs. The almost linear correlation observed confirms that the orbital interaction plays a remarkable role in this kind of process. In a general sense, the higher the energy of the substrate's orbital involved in the transition structure, the lower the activation free energy. However, the same correlation does not hold for the electronic character of the reaction. TS2 and TS4 are associated with the most electrophilic processes and exhibit the lowest activation energies. On the other hand, the oxidation of the alkenyl group (via TS1, TS3, and TS5) is a more electrophilic process than the oxidation of the sulfinyl group (via TS6 and TS7), but the activation energies for TS1, TS3, and TS5 are larger than those for TS6 and TS7.

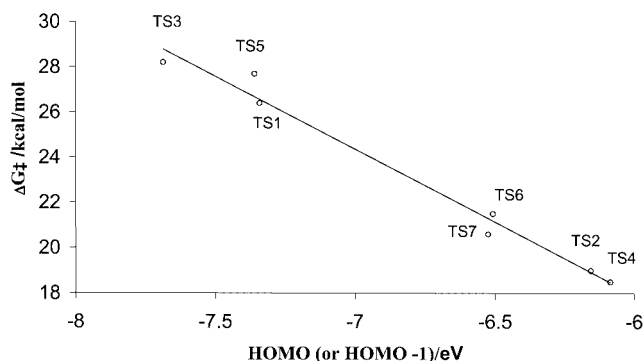


Figure 6. Calculated activation free energy ΔG^\ddagger as a function of the energy of the substrate's orbital involved in the predominant orbital interaction in the corresponding transition structures. For TS2, TS3, TS4, TS6 and TS7 the relevant substrate's orbital is its HOMO, whereas in TS1 and TS5 it is the HOMO-1.

The withdrawing effect of the allyl group makes the $\pi(\text{C}-\text{C})$ orbital in the allyl methyl sulfide higher in energy than in the ethylene molecule, so TS1 features a smaller activation energy than TS3. Conversely, the orbital related to the lone pair of the sulfur atom is lower in energy in allyl methyl sulfide than in dimethyl sulfide and, as a consequence, TS2 features a higher activation energy than TS4.

It should be mentioned that the electronic chemical potential^[21,22] of the sulfoxide molecule is calculated to be lower than that of the sulfide molecule. This indicates that the withdrawing effect of the allyl group is stronger toward the sulfur group of the unsaturated sulfide than toward the sulfinyl group of the corresponding sulfoxide. Therefore, the energy of the $\pi(\text{C}-\text{C})$ orbital in allyl methyl sulfide is greater

than in allyl methyl sulfoxide. This effect accounts for the higher activation energy demanded by TS5 than by TS1. Some departure from the linear correlation is also observed in TS5. This may be understood in terms of the orbital composition of the allyl methyl sulfoxide's HOMO-1. While in allyl methyl sulfide the HOMO-1 is clearly associated with the $\pi(\text{C}-\text{C})$ orbital, in allyl methyl sulfoxide it is an admixture of $\pi(\text{C}-\text{C})$ and oxygen p states. However, the $\pi(\text{C}-\text{C})$ orbital is also found to be the dominant orbital contribution in HOMO-2, so a close correlation between ΔG^\ddagger and the energy of $\pi(\text{C}-\text{C})$ state does not hold. Indeed, the oxygen transfer reaction taking place via TS5 ($d/b = 1.70$) is a less electrophilic process than those via TS1 ($d/b = 1.89$) and TS3 ($d/b = 1.79$).

Conclusions

Our quantum mechanical calculations have clearly elucidated the reasons why, as recently observed in experiments, unsaturated sulfides are oxidized by oxodiperoxo molybdenum complexes to sulfoxides, and subsequently to sulfones without concomitant epoxidation of the double bond. A lower free activation energy for oxidation in the sulfur center than in the double bond moiety explains the chemoselectivity of the oxidation of unsaturated sulfides/sulfoxides mediated by the peroxomolybdenum complexes.

The interaction between the $\sigma^*(\text{O}-\text{O})$ orbital of the metal peroxy oxidant and the HOMOs (related to the sulfur's lone pair) of the unsaturated sulfides is the predominant orbital interaction in the TS yielding the corresponding sulfoxides. In contrast, in the TS yielding the corresponding epoxides, the $\sigma^*(\text{O}-\text{O})$ orbital interacts with the HOMO-1 (associated with the $\pi(\text{C}-\text{C})$ bond) of the unsaturated sulfides. Therefore, the difference in energy between the orbitals associated with the sulfur's lone pair and those associated with the $\pi(\text{C}-\text{C})$ bond of a given unsaturated sulfide accounts for the more favorable oxidation of the sulfur group.

The level of chemoselectivity is predicted to diminish with increasing solvent polarity.

Experimental Section

Computational Data: Calculations based on density functional theory (DFT) were performed at the B3LYP level^[23] as implemented in the Gaussian98 program.^[24] The standard 6-311+G(2df,2p) basis set was employed to represent the H, C, O, P, and S atoms. To represent the Mo center a valence basis set (8s6p7d2f), customized by applying the generator coordinate method,^[9p] was used in conjunction with the quasi-relativistic effective core potential of Hay and Wadt.^[25] All geometry optimizations of minima and transition structures (TSs) were performed without any symmetry constraints and all stationary points were characterized by the calculation of vibrational frequencies. Wavefunctions related to TSs were checked for stability under default perturbations controlled by the *stable* directive of the Gaussian program. Starting with the TS geometries, calculations of the Intrinsic Reaction Coordinates (IRC) were carried out in order to identify the respective reactants and products.^[26] Activation parameters were

calculated on the assumption of ideal gas behavior from the harmonic frequencies, and moments of inertia by standard methods, at 298.15 K. Donor–acceptor interactions in the transition structures were examined by the Charge Decomposition Analysis (CDA) Scheme^[27] as implemented in the CDA2.1 program.^[28] Atomic charges were computed within the natural atomic orbitals framework (NBO).^[29] Long-range electrostatic solvent effects were treated with the IEF–PCM method (integral equation formalism, polarized continuum model).^[17]

Supporting Information: Cartesian coordinates and sums of electronic and thermal free energies of reactants, products, and corresponding transition states.

Acknowledgments

The authors wish to thank Q. B. Cass, M. Z. Hernandez, R. L. Longo, and F. Batigallia for helpful discussions. F. R. S. thanks the Brazilian research funding agency (FAPESP) for a postdoctoral grant. J. A. and V. S. S. acknowledge the Generalitat Valenciana, Grupos de Investigación, Proyecto GRUPOS 04/28. This study was also supported by the “Programa de Cooperação Internacional” maintained by CAPES (Brazil) and the Ministerio de Educación y Cultura del Gobierno Español. The authors are indebted to the Servei d’Informàtica of the Universitat Jaume I for providing them with excellent computer facilities.

- [1] a) S. Oae, *Organic Sulfur Chemistry: Structure and Mechanism*, CRC, Boca Raton, FL, **1991**; b) M. C. Carreño, *Chem. Rev.* **1995**, *95*, 1717–1760; c) E. N. Prilezhaeva, *Russ. Chem. Rev.* **2001**, *70*, 897–920, and references therein.
- [2] F. Batigallia, M. Zaldini-Hernandes, A. G. Ferreira, I. Malvestiti, Q. B. Cass, *Tetrahedron* **2001**, *57*, 9669–9676.
- [3] H. Mimoun, *Angew. Chem. Int. Ed. Engl.* **1982**, *21*, 734–750.
- [4] G. Keilen, T. Benneche, K. Gaare, K. Undheim, *Acta Chem. Scand.* **1992**, *46*, 867–871.
- [5] F. R. Fronczek, R. L. Luck, G. Wang, *Inorg. Chem. Commun.* **2002**, *5*, 384–387.
- [6] S. Das, T. Bhowmick, T. Punniyamurthy, D. Dey, J. Nath, M. K. Chaudhuri, *Tetrahedron Lett.* **2003**, *44*, 4915–4917.
- [7] For reviews, a) K. A. Jorgensen, *Chem. Rev.* **1989**, *89*, 431–458; b) M. H. Dickman, M. T. Pope, *Chem. Rev.* **1994**, *94*, 569–584.
- [8] For prominent examples, see: a) A. Arcoria, F. P. Ballistreri, G. A. Tomaselli, F. Di Furia, G. Modena, *J. Org. Chem.* **1986**, *51*, 2374–2376; b) J.-Y. Piquemal, S. Halut, J.-M. Brégeault, *Angew. Chem. Int. Ed. Engl.* **1998**, *37*, 1146–1149; c) G. Wahl, D. Kleinhenz, A. Schorm, J. Sundermeyer, R. Stowasser, C. Rummey, G. Bringmann, C. Fickert, W. Kiefer, *Chem. Eur. J.* **1999**, *5*, 3227–3251; d) J. M. Mitchell, N. S. Finney, *J. Am. Chem. Soc.* **2001**, *123*, 862–869; e) M. Jia, W. R. Thiel, *Chem. Commun.* **2002**, 2392–2393; f) F. E. Kühn, M. Groarke, E. Benze, E. Herdtweck, A. Prazeres, A. M. Santos, M. J. Calhorda, C. C. Romão, I. S. Gonçalves, A. D. Lopes, M. Pillinger, *Chem. Eur. J.* **2002**, *8*, 2370–2383; g) M. Jia, W. R. Thiel, *Chem. Commun.* **2002**, 2392–2393.
- [9] a) K. A. Jorgensen, R. Hoffmann, *Acta Chem. Scand. B* **1986**, *40*, 411–419; b) M. Filatov, K. Shalyaev, E. Talsi, *J. Mol. Catal.* **1994**, *87*, L5–L9; c) L. Salles, J.-Y. Piquemal, R. Thouvenot, C. Minot, J.-M. Brégeault, *J. Mol. Catal. A* **1997**, *117*, 375–387; d) D. V. Deubel, J. Sundermeyer, G. Frenking, *J. Am. Chem. Soc.* **2000**, *122*, 10101–10108; e) D. V. Deubel, G. Frenking, H. M. Senn, J. Sundermeyer, *Chem. Commun.* **2000**, 2469–2470; f) D. V. Deubel, J. Sundermeyer, G. Frenking, *Inorg. Chem.* **2000**, *39*, 2314–2320; g) C. Di Valentin, P. Gisdakis, I. V. Yudanov, N. Rösch, *J. Org. Chem.* **2000**, *65*, 2996–3004; h) I. V. Yudanov, C. Di Valentin, P. Gisdakis, N. Rösch, *J. Mol. Catal. A* **2000**, *158*, 189–197; i) A. Hrock, G. Gemmecker, W. Thiel, *Eur. J. Inorg. Chem.* **2000**, *5*, 1107–1114; j) P. Macchi, A. J. Schultz, F. K. Larsen, B. B. Iversen, *J. Phys. Chem. A* **2001**, *105*, 9231–9242; k) D. V. Deubel, J. Sundermeyer, G. Frenking, *Eur. J. Inorg. Chem.* **2001**, 1819–1827; l) D. V. Deubel, J. Sundermeyer, G. Frenking, *Org. Lett.* **2001**, *3*, 329–332; m) D. V. Deubel, *J. Phys. Chem. A* **2001**, *105*, 4765–4772; n) F. R. Sensato, Q. B. Cass, E. Longo, J. Zuckerman-Schpector, R. Custodio, J. Andrés, M. Zaldini-Hernandes, R. L. Longo, *Inorg. Chem.* **2001**, *40*, 6022–6025; o) P. Gisdakis, I. V. Yudanov, N. Rösch, *Inorg. Chem.* **2001**, *40*, 3755–3765; p) F. R. Sensato, R. Custodio, Q. B. Cass, E. Longo, M. Zaldini-Hernandes, R. L. Longo, J. Andres, *J. Mol. Struct. (Theochem)* **2002**, *589–590*, 251–264; q) D. V. Deubel, G. Frenking, P. Gisdakis, W. A. Hermann, N. Rösch, J. Sundermeyer, *Acc. Chem. Res.* **2004**, *37*, 645–652.
- [10] K. B. Sharpless, J. M. Townsend, D. R. Williams, *J. Am. Chem. Soc.* **1972**, *94*, 295–296.
- [11] a) S. Campestrini, V. Conte, F. Di Furia, G. Modena, O. Bortolini, *J. Org. Chem.* **1988**, *53*, 5721–5724; b) F. P. Ballistreri, G. A. Tomaselli, R. M. Toscano, V. Conte, F. Di Furia, *J. Am. Chem. Soc.* **1991**, *113*, 6209–6212; c) F. P. Ballistreri, A. Basso, G. Tomaselli, R. M. Toscano, *J. Org. Chem.* **1992**, *57*, 7074–7077; d) F. P. Ballistreri, G. A. Tomaselli, R. M. Toscano in *Organic reactivity: physical and biological aspects* (Eds.: B. T. Golding, R. J. Griffin, H. Maskill), Cambridge, **1995**, pp. 429–436; e) M. Bonchio, V. Conte, M. A. De Concilis, F. Di Furia, F. P. Ballistreri, G. A. Tomaselli, R. M. Toscano, *J. Org. Chem.* **1995**, *60*, 4475–4480.
- [12] D. Balcells, F. Maseras, A. Lledós, *J. Org. Chem.* **2003**, *68*, 4265–4272.
- [13] F. R. Sensato, R. Custodio, E. Longo, V. S. Safont, J. Andres, *J. Org. Chem.* **2003**, *68*, 5870–5874.
- [14] a) W. Adam, W. Hase, B. B. Lohray, *J. Am. Chem. Soc.* **1991**, *113*, 6206–6208; b) W. Adam, D. Golsch, F. C. Gorth, *Chem. Eur. J.* **1996**, *2*, 255–258.
- [15] A six-coordinate complex model was selected rather than a seven-coordinate one, because Mimoun’s complexes are known to be promptly dehydrated and the resulting forms are believed to be the ultimate reactive species.^[3]
- [16] P. Gisdakis, S. Antonczak, S. Köstlmeier, W. A. Herrmann, N. Rösch, *Angew. Chem. Int. Ed. Engl.* **1998**, *37*, 2211–2214.
- [17] a) M. T. Cancès, B. Mennucci, J. Tomasi, *J. Chem. Phys.* **1997**, *107*, 3032–3041; b) B. Mennucci, J. Tomasi, *J. Chem. Phys.* **1997**, *106*, 5151–5158; c) B. Mennucci, E. Cancès, J. Tomasi, *J. Phys. Chem. B* **1997**, *101*, 10506–10517; d) J. Tomasi, B. Mennucci, E. Cancès, *J. Mol. Struct. (Theochem)* **1999**, *464*, 211–226; e) M. Cossi, G. Scalmini, N. Rega, V. Barone, *J. Chem. Phys.* **2002**, *117*, 43–54.
- [18] O. Bortolini, V. Conte, F. Di Furia, G. Modena, *J. Mol. Catal.* **1983**, *19*, 331–343.
- [19] P. Gisdakis, N. Rösch, *Eur. J. Org. Chem.* **2001**, 719–723.
- [20] F. E. Kühn, A. M. Santos, P. W. Roesky, E. Herdtweck, W. Scherer, P. Gisdakis, I. V. Yudanov, C. Di Valentin, N. Rösch, *Chem. Eur. J.* **1999**, *5*, 3603–3615.
- [21] R. G. Parr, W. Yang, *Density Functional Theory of Atoms and Molecules*, Oxford University Press, New York, **1989**.
- [22] The electronic chemical potential (μ) is calculated as $(\epsilon_H + \epsilon_L)/2$, where ϵ_H and ϵ_L are the one-electron levels of the HOMO and LUMO frontier molecular orbitals, respectively. Such an index (μ) is used as a natural descriptor of charge transfer, as it measures the escaping tendency (or fugacity) of electrons from the atomic or molecular system.
- [23] a) A. D. Becke, *Phys. Rev. A* **1988**, *38*, 3098–3100; b) A. D. Becke, *J. Chem. Phys.* **1993**, *98*, 5648–5642.
- [24] M. J. Frisch, G. W. Trucks, H. B. Schlegel, G. E. Scuseria, M. A. Robb, J. R. Cheeseman, V. G. Zakrzewski, J. A. Montgomery, R. E. Stratmann, J. C. Burant, S. Dapprich, J. M. Millam, A. D. Daniels, K. N. Kudin, M. C. Strain, O. Farkas, J. Tomasi, V. Barone, M. Cossi, R. Cammi, B. Mennucci, C. Pom-

- elli, C. Adamo, S. Clifford, J. Ochterski, G. A. Petersson, P. Y. Ayala, Q. Cui, K. Morokuma, D. K. Malick, A. D. Rabuck, K. Raghavachari, J. B. Foresman, J. Cioslowski, J. V. Ortiz, B. B. Stefanov, G. Liu, A. Liashenko, P. Piskorz, I. Komaromi, R. Gomperts, R. L. Martin, D. J. Fox, T. Keith, M. A. Al-Laham, C. Y. Peng, A. Nanayakkara, C. Gonzalez, M. Challacombe, P. M. W. Gill, B. Johnson, W. Chen, M. W. Wong, J. L. Andres, C. Gonzalez, M. Head-Gordon, E. S. Replogle, J. A. Pople, Gaussian98, Revision A.7; Gaussian Inc., Pittsburgh, PA, **1998**.
- [25] P. J. Hay, W. R. Wadt, *J. Chem. Phys.* **1985**, *82*, 299–310.
- [26] C. Gonzalez, H. B. Schlegel, *J. Chem. Phys.* **1989**, *90*, 2154–2161.
- [27] S. Dapprich, G. Frenking, *J. Phys. Chem.* **1995**, *99*, 9352–9362.
- [28] S. Dapprich, G. Frenking, CDA 2.1, Marburg, **1994**. The program is available at <ftp://chemie.uni-marburg.de/pub/cda>.
- [29] a) A. E. Reed, R. B. Weinstock, F. Weinhold, *J. Chem. Phys.* **1985**, *83*, 735–746; b) A. E. Reed, L. A. Curtiss, F. Weinhold, *Chem. Rev.* **1988**, *88*, 899–926.

Received: January 06, 2005